# Analysis of Mesostructure Unit Cells Comprised of Octet-truss Structures

Scott R. Johnston[*], Marques Reed[*], Hongqing V. Wang[†], and David W. Rosen[*]

[*]The George W. Woodruff School of Mechanical Engineering,
Georgia Institute of Technology, Atlanta, GA 30332
[†]R&D Group, IronCAD, 700 Galleria Pkwy, Atlanta, GA 30339

**Abstract**:
A unit truss finite element analysis method allowing non-linear deformation is employed to analyze a unit cell comprised of $n^3$ octet-truss structures for their stiffness and displacement compared to their relative density under loading. Axial, bending, shearing, and torsion effects are included in the analysis for each strut in the octet-truss structure which is then related to the mesostructure level (unit cell). The versatility of additive manufacturing allows for the fabrication of these complex unit cell truss structures which can be used as building blocks for macro-scale geometries. The finite element calculations are compared to experimental results for samples manufactured on a Stereolithography Apparatus (SLA) out of a standard resin.

## 1 Introduction

Lightweight compliant structures are becoming more desirable in many areas of industry due to the advancements in manufacturing methods that are now capable of fabricating their complex geometries. Components with an internal truss structure designed for specific loading applications is an example of a lightweight structure. The automotive and aerospace industries are very interested in lightweight structures because lightweight structures can improve their product's performance. Truss structure applications have been limited in the past because of the large cost required for fabrication, or the structure was impossible to fabricate using traditional manufacturing methods. Additive manufacturing is now capable of fabricating lightweight truss structures, possibly with similar mechanical properties to conventional manufactured components with the same exterior component design.

The initial steps for introduction of truss structures in commercial applications requires mechanical analysis of the capabilities of the truss structures to determine their mechanical properties. This will allow designers to choose truss designs with knowledge of their strength, stiffness, and weight. Since truss structures are a series of struts and nodes, they behave differently from solid components. The development of fast computing systems has allowed Finite Element Analysis (FEA) to become a standard method for component design analysis, but most FEA codes usually use elements discretely in the form of beams, rods, plates, or solid elements. The nodes of the truss structures physically possess the loading constraints (tensile, compression, torsion, elongation, and buckling) of many different types of the aforementioned element types, but an element possessing all of the unique loading conditions which a truss structure node experiences does not currently exist.

A unit truss approach FEA program has been developed at Georgia Tech [1] to specifically analyze complex truss structures (described in more detail in Section 2.4) which includes tensile, compressive, torsion, and buckling effects due to structural loading. The unit truss FEA analysis is compared to experimental results for stiffness and displacement for a specified relative density of a unit cell. Each unit cell contains a different number of octet truss structures [2] possessing

the same relative density of $\bar{\rho} = 0.35$. A comparison of experimental and unit truss FEA approach are presented in Section 3.4.

## 2 Meso-structure design analysis of components

Components can be geometrically decomposed into smaller elements for analytical purpose which is precisely the analytical process employed by Finite Element Analysis (FEA). The same idea can be used to successively decompose a component (macro-scale) into medium sized elements (meso-scale) which is further subdivided into smaller building blocks (micro-scale). This decomposition ideology is the basis for the unit cell design and analysis approach to lightweight components by using truss structures within the unit cells.

### 2.1 Unit cell approach for component design

A multi-scale design approach is employed to create an appropriate truss structure for specific component geometries. The geometric design of the component can be decomposed into mesostructure unit cells (structures possessing feature sizes between micro and macro-scales as displayed in Figure 1a) such that the mesostructures are used as the basic building blocks for the component geometry. Each mesostructure unit cell is further decomposed into smaller truss structures (Figure 1c) where the octet-truss structure (Figure 1b) has been chosen to be the building block for each unit cell [3] because the mechanical behavior of the struts (lattice structure) can be predicted more readily than materials with random voids, such as foams. Performing this decomposition creates a transition from a macro scale (the component level) to a meso-scale (unit cell) and finally to the micro-scale (octet-truss). An example of this decomposition is displayed in Figure 1 to illustrate the multi-scale analysis of the component.

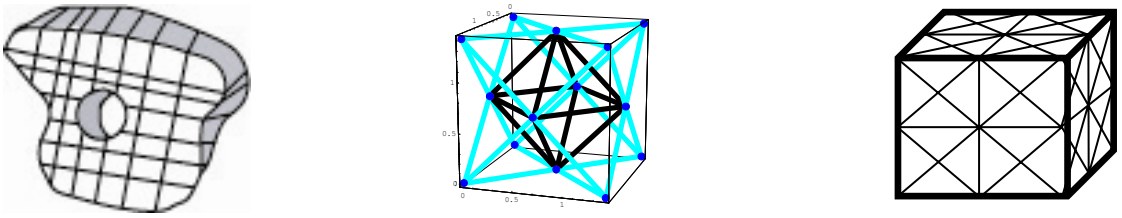

(a) (b) (c)

Figure 1. (a) Component geometry decomposed into unit cells, (b) octet-truss structure, and (c) a unit cell containing a 2x2x2 octet-truss structure.

There are many reasons for employing the unit cell design methodology. First, by using unit cells with known mechanical behavior, the unit cells can be used as an element type in a Finite Element Analysis (FEA) which reduces the computational intensity of the FEA calculations compared to the current FEA definition of numerous nodes and struts comprising the truss structure. A second advantage in using this mesostructure approach provides the designer local control of the mechanical behavior at the component level by altering the composition of the unit cells at the mesostructure level. This advantage also allows for a maximum component performance with respect to weight under defined loading conditions because less dense unit cells may be used in locations that carry less of the applied load.

The following investigation of unit cells comprised of arrays of octet-truss structures will expand upon previous research of the octet-truss structure by: (1) including bending, shearing, and torsion effects in addition to the tensile effects and (2) analysis of arrays of octet-truss

structures that include the interaction between neighboring octets. This additional information about unit cell octet-truss structures provides necessary information to create a unit cell library to construct macro level component geometries.

### 2.2 Octet-truss structure analysis

The octet-truss structure (displayed in Figure 1b) was chosen as the building block for the unit cells because of a previous analysis of the structure [2] and its good mechanical properties under most types of loading conditions. The initial analysis of the octet-truss structure was performed by Deshpande, Fleck, and Ashby [2] where their analysis rigorously studied the octahedral portion (Figure 2a) of the octet-truss structure for stiffness, compliance, and buckling. They state that the octahedral portion of the octet-truss structure will contribute the majority of the stiffness of the structure under compressive loading. Therefore their analysis is restricted to the octahedral section of the octet-truss structure and does not include the tetrahedral section of the structure (black section displayed in Figure 2b).

Herein, a further analysis of the octet-truss structure is presented that includes the eight tetrahedrons of the octet structure for compliance. Both of these algebraic presentations consider each strut to be pinned at their respective nodes. An algebraic formulation for struts that are fully constrained at each node becomes too complex when all of the loading conditions (tensile, bending, shear, and torsion) are included and will not be presented.


(a) (b)

Figure 2. (a) Octahedral section of the octet-truss structure (red inner section) and (b) octet-truss structure with highlighted a corner tetrahedron section (black section).

The relative density of a unit cell will be used as a metric for characterization of the mechanical behavioral properties of the cell. The unit cell's relative density is determined by the thickness of each octet-truss strut and number of octet-truss structures located within the cell defined by

$$\overline{\rho} = 6\pi\sqrt{2}\left(\frac{a}{l}\right)^2 \tag{1}$$

where $a$ is the strut diameter and $l$ is the length of each strut. Equation 1 represents the material volume of the inscribed unit cell containing an octet-truss structure, specifically, only half of the volume of each strut on each of the six faces is included because the remaining volume lies in the volume for adjacent cells. Each unit cell is analyzed for its stiffness (compliance) with respect to

the relative density. Unit cells containing $n$ x $n$ x $n$ arrays of octet-truss structures are also be analyzed (for $n$ = 1,2,3).

Previous investigations of the octet-truss structure by Deshpande, Fleck, and Ashby [2] assumed that each node of the structure was pinned and free to rotate about the node, thus assuming only tensile conditions are present within the struts (struts are either in tension or compression). Additionally, their analysis primarily involved investigation of failure of the octet-truss structures due to elastic buckling or plastic collapse. Thus, bending moments, shearing forces, and torsion effects were not included within their analysis.

### 2.2.1 Octahedral structure analysis

Deshpande, Fleck, and Ashby [2] have determined that the octahedral section of the octet-truss structure (displayed in Figure 2a) determines the stiffness for the entire truss structure. For their analysis, they assume that all of the joints are pinned and only axial forces are present within the struts of the octahedral section. The compliance matrix for only the *octahedral* structure is isotropic [4] and is determined algebraically to be

$$\begin{Bmatrix} \varepsilon_x \\ \varepsilon_y \\ \varepsilon_z \\ \varepsilon_{yz} \\ \varepsilon_{xz} \\ \varepsilon_{xy} \end{Bmatrix} = \begin{bmatrix} s_1 & -s_2 & -s_2 & 0 & 0 & 0 \\ & s_1 & -s_2 & 0 & 0 & 0 \\ & & s_1 & 0 & 0 & 0 \\ & & & s_3 & 0 & 0 \\ & sym & & & s_3 & 0 \\ & & & & & s_3 \end{bmatrix} \cdot \begin{Bmatrix} \sigma_x \\ \sigma_y \\ \sigma_z \\ \sigma_{yz} \\ \sigma_{xz} \\ \sigma_{xy} \end{Bmatrix} \tag{2}$$

and expressed in matrix form

$$\{\bar{\varepsilon}\} = [C] \cdot \{\bar{\sigma}\} \tag{3}$$

where

$$s_1 = \frac{3\sqrt{2}}{4\pi}\left(\frac{l}{a}\right)^2 \frac{1}{E_s} = \frac{9}{\bar{\rho}}\frac{1}{E_s} \tag{4a}$$

$$s_2 = \frac{\sqrt{2}}{4\pi}\left(\frac{l}{a}\right)^2 \frac{1}{E_s} = \frac{3}{\bar{\rho}}\frac{1}{E_s} \tag{4b}$$

and

$$s_3 = \frac{\sqrt{2}}{2\pi}\left(\frac{l}{a}\right)^2 \frac{1}{E_s} = \frac{6}{\bar{\rho}}\frac{1}{E_s} \tag{4c}$$

where $E_s$ is the elastic modulus for the solid strut material. (Note that $s_3$ in Equation 4c is different than printed in [2], we believe that there is a typographical error in the publication.) The compliance matrix [$C$] stated in Equation 3 is for a pinned node octahedral structure (Figure 2a) and not the entire octet-truss structure (Figure 2b). Deshpande's analysis uses the compliance matrix [$C$] to determine the stiffness of the octet-truss and then makes a comparison to FEA results. The eight tetrahedral structures that are required in conjunction with the octahedral structure to create the octet-truss structure are not included in these calculations and are not represented in Equations 2-4.

### 2.2.2 Pinned octet truss structure analysis

The authors concur with Deshpande that the majority of the compressive or tensile loads are absorbed within the octahedral section of the of the octet-truss structure, but the tetrahedral elements at the corners also contribute to the compliance or stiffness of the complete octet structure. This is especially true when analyzing arrays of octet-truss structures, which will be illustrated in the following sections.

The direct stiffness method can be used to determine the compliance matrix and reproduce Equations 2-4 for a pinned node octet-truss structure [3]. The compliance matrix $[\overline{C}]$ for the octet-truss structure has the same matrix equation

$$\{\bar{\varepsilon}\} = \left[\overline{C}\right] \cdot \{\bar{\sigma}\} \tag{5}$$

where the octet compliance matrix $[\overline{C}]$ for a pinned node *octet*-truss structure (Figure 2b) in Equation 5 has the same matrix structure as Equation 2 with the $s_i$ values in Equation 4 replaced by the $\bar{s}_i$ values presented in Equation 6a-c which have been algebraically determined

$$\bar{s}_1 = \frac{1}{\pi}\left(\frac{l}{a}\right)^2 \frac{1}{E_s} = \frac{6\sqrt{2}}{\bar{\rho}} \frac{1}{E_s} \tag{6a}$$

$$\bar{s}_2 = \frac{1}{3\pi}\left(\frac{l}{a}\right)^2 \frac{1}{E_s} = \frac{2\sqrt{2}}{\bar{\rho}} \frac{1}{E_s} \tag{6b}$$

and

$$\bar{s}_3 = s_3 = \frac{\sqrt{2}}{2\pi}\left(\frac{l}{a}\right)^2 \frac{1}{E_s} = \frac{6}{\bar{\rho}} \frac{1}{E_s} \tag{6c}$$

The inclusion of the eight tetrahedrons at the corners of the octahedral structure (thus creating the octet structure) does effect the compliance matrix [*C*], specifically, the $s_1$ and $s_2$ terms. The coefficient for $s_1$ decreased from 9 to $6\sqrt{2} \approx 8.49$ (octahedral to octet structure) and the $s_2$ decreased from 3 to $2\sqrt{2} \approx 2.83$, both decreasing by ~5%). The decrease in the compliance coefficients implies that the octet structure is less compliant (or more stiff) than the octahedral structure (along the principle load axis) and in transverse directions under loading (see Figure 6a). The shearing term $s_3$ did not change between the octahedral and octet analysis because the twisting effect of the octet truss structure was not constrained to remain planar under the applied shearing load (i.e., the corner nodes were allowed to move out of plane due to the twisting nature of the shearing force). Since this was only an analysis of a single octet, the shearing effect will become more significant when the octet structures are combined to create arrays of octets (i.e., unit cells).

### 2.3 Unit truss Finite Element Analysis (FEA) approach

Unit cells comprised of octet truss structures are currently being analyzed using a unit-truss finite element analysis program in MATLAB that has been developed at Georgia Tech [1]. The unit-truss finite element program is capable of non-linear analysis, but for the current stage in this project, only linear elastic behavior is considered. The FEA program includes axial, bending, shearing, and torsion effects that are present in loading of the octet truss structure where previous analyses only included axial effects [2]. A discussion of the effective mechanical behavior of the unit cells using the unit truss FEA program will be discussed.

In the unit truss approach, a unit truss is used as a new unit cell for mechanics analysis of cellular structures, including lightweight structures, and compliant mechanisms. A unit truss consists of a central node and a set of half-struts that are connected to the node. Every two neighboring unit trusses share a common strut. An example of unit trusses is shown in Figure 3.

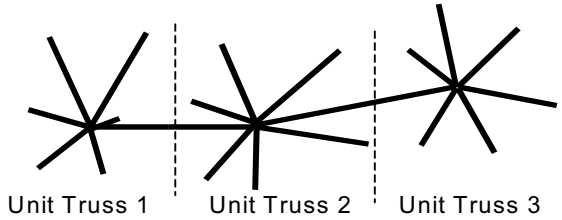


Figure 3. Series of three unit truss structures that are connected between each node.

Unit trusses can be parameterized, analyzed, patterned, and manufactured to support the desired design. In a unit truss, the strain and stress around the nodes (displayed in Figure 4), are usually complicated due to considerable inter-strut interactions and large bending moments [1]. The unit truss is leveraged from the ground truss approach and homogenization method [5, 6]. The constitutive equations of 2-D and 3-D unit trusses are shown in Equations 7-9. The linear elasticity of a unit truss is represented by $\underset{\sim}{K}_e$, while $\underset{\sim}{U}$ and $\underset{\sim}{F}$ represent the nodal displacements and forces. Unit trusses can have any number of incident struts and they are special finite elements for analyzing large cellular structures.

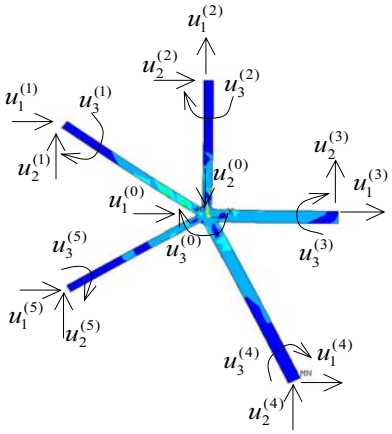


Figure 4. Unit truss nodal degrees of freedom for a unit truss node with five attached struts.

Static equilibrium: $\underset{\sim}{K}_e \cdot \underset{\sim}{U} = \underset{\sim}{F}$ (7)

Stiffness: $$\left[\underset{\sim}{K}_e\right] = \begin{bmatrix} \sum_{i=1}^{N} \Phi_{11}^{(i)} & \Phi_{12}^{(1)} & \Phi_{12}^{(2)} & \cdots & \Phi_{12}^{(N)} \\ \Phi_{21}^{(1)} & \Phi_{22}^{(1)} & 0 & \cdots & 0 \\ \Phi_{21}^{(2)} & 0 & \Phi_{22}^{(2)} & \cdots & 0 \\ \vdots & \vdots & \vdots & \ddots & \vdots \\ \Phi_{21}^{(N)} & 0 & 0 & \cdots & \Phi_{22}^{(N)} \end{bmatrix}_{3(N+1)\times 3(N+1)} \quad (8)$$

$$\text{Nodal Displacements:} \quad [\underset{\sim}{U}] = \left[ \left[ \underset{\sim}{u}^{(0)} \right] \ \left[ \underset{\sim}{u}^{(1)} \right] \ \cdots \ \left[ \underset{\sim}{u}^{(N)} \right] \right]^T$$
$$\text{Nodal forces:} \quad [\underset{\sim}{F}] = \left[ \left[ \underset{\sim}{f}^{(0)} \right] \ \left[ \underset{\sim}{f}^{(1)} \right] \ \cdots \ \left[ \underset{\sim}{f}^{(N)} \right] \right]^T \tag{9}$$

A unit truss can be manufactured, whereas the microstructure for homogenization can not be physically fabricated because homogenization is an artificial representation. Using the unit truss approach, combined with the tangent stiffness method, truss structures can be analyzed under axial forces, bending, torsion, nonlinearity, and buckling [7].

### 2.4 Unit cells comprised of octet truss structures

The unit cell analysis will be applied to three different types of unit cells that are comprised of octet-truss structures, displayed in Figure 5. The analysis is based on the approach used by Deshpande by relating the relative stiffness ($E/E_s$) to the relative density ($\overline{\rho}$ in Equation 1) for a fixed sized unit cell. The relative density for a unit cell geometry is altered by varying the diameter of the struts of the octet-truss structure. Unit cells comprised of a single octet, a 2x2x2 array, and a 3x3x3 array are analyzed within this work, but this analysis can easily be expanded to arbitrary unit cells and octet arrays.

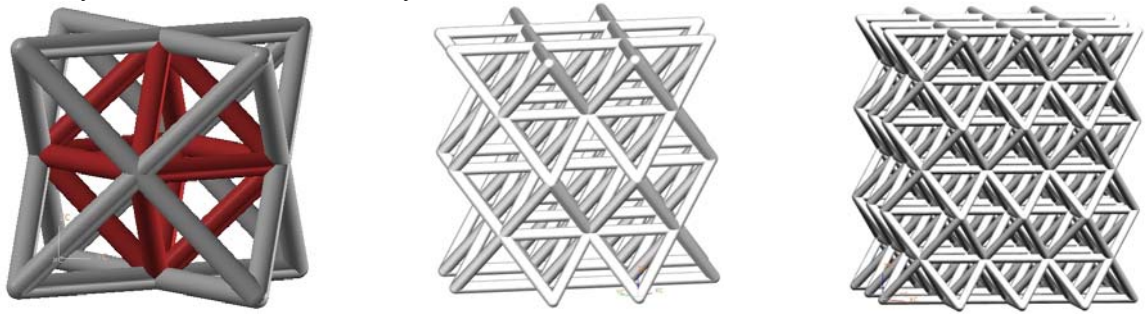

(a) (b) (c)

Figure 5. CAD images of unit cells comprised of octet-truss structure, (a) single octet, (b) 2x2x2 array of octets, and (c) 3x3x3 array of octets.

### 2.5 Unit truss FEA analysis of unit cells

A direct comparison of the relative stiffness of unit cells that are composed a single octet and an array of octet-truss structures is presented herein. To maintain uniformity between analyses of the different mesostructures (unit cells constructed from an array of octets), the dimension of the unit cell is set to a fixed value and the applied compressive load is appropriately distributed to each node creating the same uniform applied stress. A comparison between the unit-truss FEA approach (described in Section 2.3) of a mesostructure unit cell and Deshpande's analysis of the octet-truss structure is detailed below. Only linear elastic deformations have been considered in this work, but the unit-truss FEA program is capable of determining non-linear deformation and buckling effects, which will be analyzed in future work.

Figure 6 displays the relative stiffness plotted with respect to the relative density of the mesostructure unit cell. An increase in the relative stiffness is observed as the relative density increases for the unit cells. To increase the relative density of the unit cell is to increase the strut diameter, and a larger diameter strut will possess a greater stiffness value that translates to the overall relative stiffness of the structure. Figure 6a displays the relative stiffness ($E/E_s$) for an

octahedral and octet truss structure (Equations 4 and 6, respectively) at the center node (point $p_c$ in Figure 2b). Note that the inclusion of the eight corner tetrahedral sections to the octahedral section to create the octet structure only slightly increases the relative stiffness of the structure as stated earlier in Section 2.2.2.

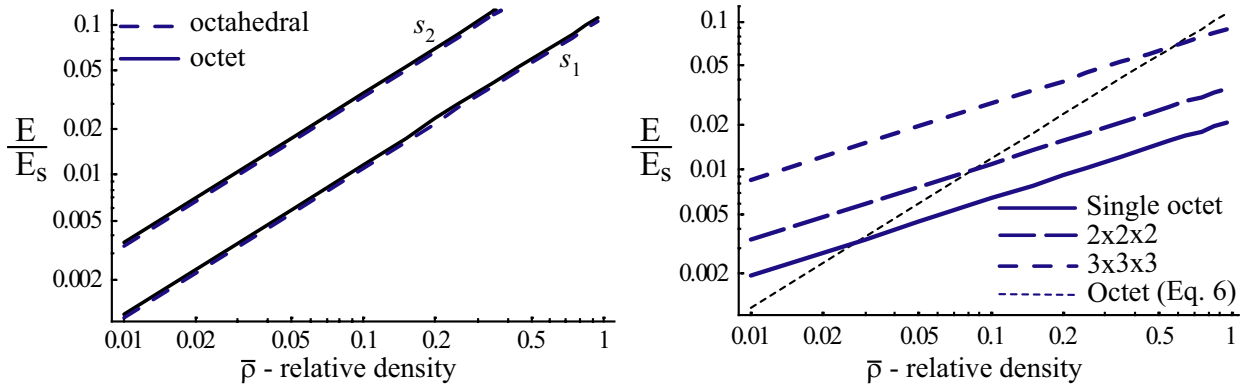


(a) (b)

Figure 6. Log-log plot of the relative stiffness ($E/E_s$) verses relative density for (a) the pinned node octahedral (Eq. 4) and octet structure (Eq. 6), and (b) the pinned node octet structure and the unit-truss FEA analysis of unit cells (analysis includes tensile, shear, bending, and torsion).

The unit-truss FEA results of unit cells comprised of a single, 2x2x2, and 3x3x3 array of octet truss structures is displayed in Figure 6b. The general trend of an increase in relative stiffness ($E/E_s$) is observed, but the unit-truss FEA results indicate that the rate of change in relative stiffness with respect to relative density is less than predicted by the algebraically determined relative stiffness (Equations 4 and 6). A comparison between Eq. 6 (valid for only a single octet) and the unit-truss FEA results for a single octet indicate that Eq. 6 predicts higher values of relative stiffness for $\overline{\rho} > 0.03$, as displayed in Figure 6b.

The unit-truss FEA results also indicate that as the number of octet truss structures increase within a fixed unit cell geometry, the relative stiffness also increases. Specifically, a unit cell with a fixed relative density has a greater relative stiffness with 27 (3x3x3) octet-truss structures (Figure 5c) when compared to the unit cell containing eight (2x2x2) octet-truss structures (Figure 5b). Therefore, unit cells comprised of octet-truss structures with a fixed relative density becomes more stiff (less compliant) when the number of octet-truss structures increases. In order to increase the number octets within the unit cell and still maintain the same relative density, the strut diameter and length must both be decreased. Indicating that the relative stiffness is more sensitive to the strut length than the strut diameter (by Equation 1). Unfortunately, this result was not observed experimentally, which is presented in Section 3.

## 3 Experimental compression tests of unit cells comprised of octet-truss structures

Unit cells comprised of octet-truss structures were fabricated and subjected to a mechanical compression test to determine their material properties. The unit cells were comprised of a single, 2x2x2, and 3x3x3 array of octet-truss structures, as displayed in Figure 5. These unit cell test specimens were created to observe the effect on the unit cell's mechanical properties with respect to the number of composing octet-truss structures. The compression test procedure for the unit cells followed the standard compression test method for determining compressive properties of rigid plastics, ASTM D 695-02a.

### 3.1 Specimen design and fabrication

A relative density value of 0.35 was chosen to compare the effect of changing the number of octet-truss structures in the unit cell. The test specimen unit cell was designed to be a 50 mm cubic cell, containing $n^3$ octet-truss structures ($n$ = 1, 2, or 3). In order to create geometric conditions as close to the octahedral analysis conducted by Deshpande [2], the octet-truss structures were arranged such that there are either 1, 8, or 27 *octahedral* structures in the unit cell (formed by the octet-truss structures). The geometry of the unit cells are displayed in Figure 5. The strut length and diameter of the octet-truss structures are calculated such that each unit cell possesses the same relative density, $\overline{\rho} = 0.35$. The average values for the overall dimensions of the three different types of unit cells is listed in Table 1. The ASTM sample specimens are right circular faced cylinders that are 25.57 mm tall with a diameter of 12.67 mm.

Table 1. Average dimension measurements of unit cell test specimens with $\overline{\rho} = 0.35$ (6 test samples for each group).

| Array Size | Strut Dia. (mm) | Height (mm) | $Width_1$ (mm) | $Width_2$ (mm) | XY Projected Area ($mm^2$) |
|---|---|---|---|---|---|
| Single | 8.14 | 58.99 | 58.82 | 58.97 | 3468.26 |
| 2x2x2 | 3.98 | 54.87 | 57.71 | 57.78 | 3334.68 |
| 3x3x3 | 2.60 | 53.59 | 50.44 | 50.47 | 2545.58 |

Table 2. Material properties of RenShape™ SL 7510 resin.

| Material Property | Value |
|---|---|
| Tensile mod. ($E_s$) | 2.634 [GPa] |
| Tensile Str. ($\sigma_Y$) | 57 [MPa] |
| Elongation at break | 10.1 % |
| Density | 1.18 [$g/cm^3$] |

The experiment specimens were manufactured on a 3D Systems SLA3500 using RenShape™ SL 7510 resin. The "exact" build style was used for specimen fabrication with a layer thickness of 0.1016 mm (0.004 in) and a beam width of 150 μm. The samples were ultrasonically cleaned in isopropyl alcohol for 10 minutes and post cured in a UV oven for 60 minutes. The samples were isolated from UV light and sealed in a plastic bag to minimize any environmental effects on the specimens before testing. The samples were tested approximately 40 days after fabrication.

### 3.2 Empirical compression measurements and results

The unit cell specimens with relative density of 0.35 exhibited both brittle and ductile failure responses. The unit cells containing a single octet and the 2x2x2 octet array both resulted in catastrophic failure with little or no audible warning before failure (complete destruction). The stress-strain curve (displayed in Figure 7) clearly shows a brittle failure response for the single octet and 2x2x2 array unit cell. The 3x3x3 octet array unit cell exhibited a more ductile failure accompanied by audible cracking before yielding. Some of the 3x3x3 octet arrays did not catastrophically fail and these specimens remained relatively intact after testing. The initial behavior of the 2x2x2 and 3x3x3 unit cells were very similar possessing almost the same stiffness (0.060 and 0.065 GPa, respectively), but the 2x2x2 had a brittle failure response while the 3x3x3 sample exhibited a more ductile failure response. The average experimental results for the unit cell octet arrays is provided in Table 3.

The amount of strain produced in the unit cells increased as the number of octet-truss structures increased, specifically from $\varepsilon_{1x} = 0.0723$ for the single to $\varepsilon_{3x} = 0.0889$ for the 3x3x3 unit cell. Ironically, the same trend can not be stated for the maximum allowed stress and unit cell stiffness. The maximum applied stress and the stiffness for the 2x2x2 octet array unit cell are less than the values for both the single and 3x3x3 octet array unit cells. The stiffness of the

3x3x3 octet array unit cell ($E_{emp}$=0.065 GPa) was significantly less stiff than the single octet unit cell ($E_{emp}$=0.107 GPa) and required approximately half of the applied load ($F_{max}$) to achieve 18% more strain than the single octet unit cell.

Table 3. Average measured and calculated values of the experimental compression test.

| Octet Array Size | $\delta_{max}$ (mm) | $F_{max}$ (kN) | $\varepsilon_{max}$ (mm/mm) | $\sigma_{max}$ (MPa) | $E_{emp}$ (GPa) | $E_{emp}/E_s$ |
|---|---|---|---|---|---|---|
| Single | 4.25 | 15.415 | 0.0723 | 4.52 | 0.107 | 0.0405 |
| 2x2x2 | 4.72 | 11.379 | 0.0854 | 3.41 | 0.060 | 0.0228 |
| 3x3x3 | 4.80 | 8.696 | 0.0889 | 3.42 | 0.065 | 0.0247 |
| ASTM Samples | 2.91 | 10.248 | 0.1137 | 81.10 | 1.801 | N/A |

Note that the stiffness for the SL 7510™ resin has been determined to be $E_{ASTM}$ = 1.801 GPa by the ASTM sample results, which is approximately 2/3 of the manufacturer's stated value of $E_s$ = 2.634 GPa (presented in Table 2). For sake of simplicity, the manufacturer's stated modulus value for Es will be used in all the following relative stiffness calculations.

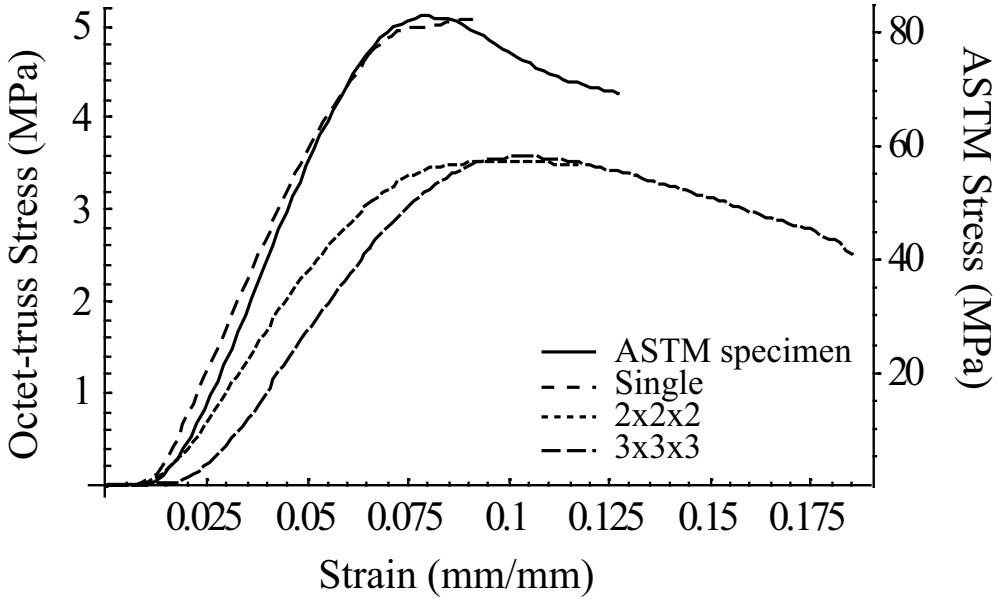


Figure 7. Stress strain plot of the compression tests for the unit cells comprised of octet-truss structures (all possessing a relative density of 0.35) and the ASTM specimens.

The single octet unit cell possessed the greatest relative stiffness ($E/E_s$) of 0.0405 (or approximately 4% of $E_s$) while the 3x3x3 possessed approximately half the stiffness of the single octet with a relative stiffness of 0.0247 (or 2.47% of $E_s$). All of the unit cell specimens experienced total displacements ranging 4.00-4.62 mm resulting from maximum loads ranging from 8.7-15.4 kN.

### 3.3 Unit truss FEA computations for unit cells comprised of octet-truss structures

A FEA simulation of the compression experiments conducted in Section 3.2 using the unit truss FEA program is presented in this section for the octet-truss structures (unit cells). The geometric parameters of the unit cells (presented in Table 1) and material properties for SL7510 resin (presented in Table 2) are used in the unit truss FEA program to produce the results

displayed in Table 4. The unit truss FEA program calculated significantly less maximum strain ($\varepsilon_{max}$) of the unit cells by two orders of magnitude.

Table 4. Unit truss FEA results for unit cells using experiment loading conditions.

| Octet Array Size | Applied Stress (MPa) | $\delta_{max}$ (mm) | $\varepsilon_{max}$ (mm/mm) | $E_{calc}$ (MPa) | $E_{calc}/E_s$ |
|---|---|---|---|---|---|
| Single | 4.445 | 2.723 | 0.0462 | 96.28 | 0.0366 |
| 2x2x2 | 3.412 | 2.813 | 0.0513 | 66.57 | 0.0253 |
| 3x3x3 | 3.416 | 2.421 | 0.0477 | 71.63 | 0.0272 |

The unit truss FEA analysis produces the same trend in relative stiffness between the unit cells that is observed experimentally. The FEA analysis has determined that the 2x2x2 octet unit cell is the most compliant (least stiff) of the octet-truss unit cells and allowing the largest amount of strain to be produced.

### 3.4 Comparison of analytical, experimental results, and ,unit truss FEA computations

A comparison of the analysis approaches of the octet-truss unit cells presented in Sections 2.2, 3.2, and 3.3 is displayed in Table 5. The relative stiffness equations (Eq. 4 and 6) are for a single truss structure (octahedral and octet, resp.) and are also used for unit cells comprised of arrays of octahedral/octet truss structures (Deshpande [2] also employed this type of scaling).

Table 5. Relative stiffness comparison between the analytical octahedral, octet, and unit-truss FEA compliance to the empirical relative stiffness results for a unit cell with $\overline{\rho} = 0.35$.

| | (Table 3) | (Eq. 4) | (Eq. 6) | (Table 4) | Relative error ($Err_{rel}$) to empirical | | |
|---|---|---|---|---|---|---|---|
| Octet Array Size | $\frac{E_{emp}}{E_s}$ | $\frac{E_{octahed}}{E_s}$ | $\frac{E_{octet}}{E_s}$ | $\frac{E_{FEA}}{E_s}$ | $\frac{E_{octahed}}{E_s}$ | $\frac{E_{octet}}{E_s}$ | $\frac{E_{FEA}}{E_s}$ |
| Single | 0.0405 | 0.0389 | 0.0412 | 0.0366 | 3.95 % | 1.73 % | 9.63 % |
| 2x2x2 | 0.0228 | 0.0389 | 0.0412 | 0.0253 | 70.6 % | 80.7 % | 10.96 % |
| 3x3x3 | 0.0247 | 0.0389 | 0.0412 | 0.0272 | 57.5 % | 66.8 % | 10.12 % |

The analytically determined relative stiffness for the octahedral and octet truss structure most accurately modeled empirical relative stiffness for the single octet unit cell (relative errors of 3.95% and 1.73%, respectively), but these analytical models significantly loose their accuracy when applied to unit cells comprised an array of truss structures (errors increased to 57-80%). Therefore these analytical models have a significant limitation in their application. The unit-truss FEA was very consistent in is predictive capability of the relative stiffness with relative errors ranging tightly about 10% for all of the unit cells analyzed. No significant accuracy was lost in changing the number of truss structures comprising the unit cells.

## 4 Conclusions

An analysis of unit cells comprised of different sizes of octet truss structures has been performed. An analytical formulation for the octet-truss structure has been presented that can more accurately predict the relative stiffness for a single octet truss structure, which has been confirmed experimentally. A unit-truss FEA program has been employed to simulate compression testing of unit cells, exhibiting an accuracy of 10% relative error to experimentation

for the relative stiffness of all of the unit cells analyzed. The unit truss FEA program shows promise as an analysis tool for unit cells comprised of arbitrary truss structures.

## 5 Future research tasks

The analysis of the octet-truss structure is the beginning of the next few steps for the mesostructure design synthesis. A library of unit cells will be created after determining the behavior of various *n* x *n* x *n* arrays of octets under different loading conditions (non-uniform loads, shearing loads, and torsion). These tasks may now progress with the knowledge that the unit-truss FEA program is capable of simulating empirical results.

The library of the mesostructure unit cells can then be used as building blocks for component geometries. An optimization program can be applied to design the component geometry for lightweight by using less dense unit cells with either greater or less stiffness where applicable due to defined loading on the component. For each loading condition, an optimization function will be used to reduce internal energy, increase strength, and reduce weight based on the application of the structure. The optimization function will accomplish this through the removal of unnecessary elements, increasing the cross-sectional area of struts with high orders of stress, and reducing the cross-sectional area of those with low orders of stress. The goal in this is to create a component comprised of unit cell truss structures that have been designed according to their required strength, flexibility, toughness, etc.

## 6 Acknowledgements

Financial support for this work has been funded by the National Science Foundation (NSF) grant DMI-0522382. The authors would like to thank the following individuals at Georgia Tech for their individual contributions to this research: Robert Cooper for helping with compression testing, and Jeff Lloyd and Amanda O'Rourke for CAD and image generation. The authors would also like to thank Professor Paul Labossiere at the University of Washington-Seattle for performing the second round of compression tests.

## References

[1] Wang H. A unit cell approach for lightweight structure and compliant mechanism. School of Mechanical Engineering, vol. Ph.D. Atlanta, GA: Georgia Institute of Technology, 2005.

[2] Deshpande VS, Fleck NA, Ashby MF. Effective properties of the octet-truss lattice material. Journal of the Mechanics and Physics of Solids 2001;49:1747.

[3] Fuller RB. Synergetic Building Construction. In: Patent U, editor. United States of America, 1961.

[4] Boresi AP, Schmidt RJ, Sidebottom OM. Advanced Mechanics of Materials: John Wiley & Sons, Inc., 1993.

[5] Bendsoe MP, Kikuchi N. Generating optimal topologies in structural design using a homogenization method. Computer Methods in Applied Mechanics and Engineering 1988;71:197.

[6] Frecker M, Ananthasuresh GK, Nishiwaki S, Kirkuchi N, Kota S. Topological systhesis of compliant mechanisms using multi-criteria optimization. ASME Journal of Mechanical Design 1997;119:238.

[7] Fu YB, Ogden RW. Nonlinear elasticity : Theory and Applications: Cambridge University Press, 2001.